Sobolev scalar products in the construction of velocity models — application to model Hess, to SEG/EAGE Salt Model, and to model Pluto 1.5

Petr Bulant

Department of Geophysics, Charles University, Ke Karlovu 3, 121 16 Praha 2, Czech Republic, Fax: +420-2-2191 1214, E-mail: bulant@seis.karlov.mff.cuni.cz

Preface

The theoretical paper by Klimeš (2000a) and the technical paper by Bulant (2000), which were published in the last Report, have been combined and considerably revised, mainly from the point of view of readability. The resulting paper (Bulant 2002), which also very briefly mentions the results of smoothing the SEG/EAGE Salt Model, have been accepted for publication in special issue of PAGEOPH to be printed approximately in June 2002.

The above mentioned paper from PAGEOPH have been supplemented with detailed description of smoothing the SEG/EAGE Salt Model and with description of smoothing model Pluto 1.5, and is presented here to the reader.

Summary

The minimization of the Sobolev norm during linearized inversion of given data enables to control the model parameters unresolved by the data being fitted. Even if a reasonably looking model can be obtained without minimizing the Sobolev norm, it may be too rough for some computational methods. We may construct models optimally smooth for given computational methods by minimizing the corresponding Sobolev norm during the inversion.

Probably the smoothest models are required by the ray methods. The efficiency of ray tracing can be evaluated in terms of the "average Lyapunov exponent" for the model. The "average Lyapunov exponent" may be approximated by the square root of the corresponding Sobolev norm of the model, which allows models most suited for ray tracing to be constructed.

Keywords

Model specification, smoothing, inversion, ray methods, Sobolev norm, Lyapunov exponent.

In: Seismic Waves in Complex 3-D Structures, Report 11 (Dep. Geophys., Charles Univ., Prague, 2001), pp. 133–159

1 Introduction

The construction of velocity models is a complex task, which covers the application of many different model building tools, including smoothing. We would like to show that one of the useful tools in the velocity model building process is the application of Sobolev scalar products.

In this paper, we shall describe the technique to take the given data, form an objective function, and build a continuous B–spline parametrized velocity (or slowness) model using the method of minimizing the selected objective function. As this is an inverse problem, we shall speak of the "inversion of the given data", or shortly "inversion". The data may be either measured travel times, values of material parameters and coordinates of points at interfaces obtained from wells, or gridded material parameters and triangulated interfaces obtained from any model building process. In principle, we treat the construction of continuous velocity models from existing gridded velocities in the same way as the linearized travel–time inversion. We would like to show that including the minimization of the corresponding Sobolev norm into the inversion of the given data allows us to construct models optimal for the selected computational method.

The Sobolev scalar product of two functions is a linear combination of the L_2 Lebesgue scalar products of the zero, first, second or higher derivatives of the functions. The linear combination should preserve the properties required of scalar products (symmetry and positiveness). The Sobolev norm of two functions is the square root of the Sobolev scalar product of the functions.

The minimization of the Sobolev norm during linearized inversion of given data enables to control the model parameters unresolved by the data being fitted. For example, if we are fitting discrete values of a material parameter with a smooth function, the properties of interpolation between the discrete values may be controlled by means of minimizing the square of the selected Sobolev norm of the function. Similarly, if we are fitting discrete values of a structural interface, the behaviour of the interpolated function between the discrete points, and also outside the region covered by the data for the interface, may be controlled by the given Sobolev norm of the function.

Even if a reasonably looking model can be obtained without minimizing the Sobolev norm, it may be too rough for some computational methods. The errors of many computational methods may be approximated by a function dependent on the Sobolev norm of functions describing the model. We may thus construct models optimally smooth for given computational methods.

Probably the smoothest models are required by the ray methods. In complex models, the number of arrivals increase rapidly with travel time. The initial–value ray tracing in such models is still possible, but the solution of boundary–value problems, e.g., two–point ray tracing, is slow and expensive due to the large number of arrivals at each receiver. We thus consider the number of arrivals to be one of the criteria of applicability of the ray methods. In complex models, the behaviour of rays becomes chaotic and the geometrical spreading, number of arrivals and density of caustic surfaces increase exponentially with travel time. The exponential increment may be described quantitatively in terms of the "average Lyapunov exponent" for the model. The "average Lyapunov exponent" may be approximated by the square root of the corresponding Sobolev norm of the model. This enables quantitative criteria on models, so as to be suitable for ray tracing, to be determined in terms of Sobolev scalar products. The criteria then allow the optimum models of geological structures for ray tracing to be constructed either by smoothing existing rough models, or by inversion of seismic data.

The construction of a model for ray methods is a typical example of using the Sobolev norm for smoothing. The task of smoothing a given rough model may be solved either as a direct problem (Grubb & Walden 1995, Versteeg 1991) by, e.g., convolution or wavenumber filtering, or as an inverse problem (Pretlová 1976, 1985) by fitting the values in the rough model with the new smooth and sparsely parametrized model. Smoothing the given model by inversion is advantageous not only because we treat the problem of model smoothing in the same way as inversion of measured data, but also because we may include the minimization of the suitable Sobolev norm into the inversion, and thus ensure the feasibility of ray tracing in the smooth model.

2 Sobolev scalar products and Sobolev norms

We define the Sobolev scalar product (see, e.g., Tarantola 1987) of functions f and g as a linear combination of the L_2 Lebesgue scalar products of the zero, first, second or higher derivatives of the functions:

$$((f,g)) = \left[\int \mathrm{d}\mathbf{x}\right]^{-1} \sum_{ij\ldots}\sum_{ab\ldots} \int \mathrm{d}\mathbf{x}\; b_{ij\ldots|ab\ldots}\; f^{*}_{,ij\ldots}(\mathbf{x})\; g_{,ab\ldots}(\mathbf{x}) \quad , \tag{1}$$

where $\int \mathrm{d}\mathbf{x}$ is the definite integral over the model volume, and $b_{ij\ldots|ab\ldots}$ are real-valued coefficients of the linear combination. Symbol $f_{,i}$ denotes the partial derivative of function f with respect to the i-th coordinate axis. The order of the considered partial derivative $f_{,ij\ldots}$ equals the number of indices $ij\ldots$. The indices take the values from 1 to 3 in 3-D, 1 to 2 in 2-D and 1 in 1-D. The linear combination should preserve the properties required of scalar products (symmetry and positiveness). The asterisk denoting complex–conjugacy is included just for completeness here; we consider real–valued functions and real–valued coefficients $b_{ij\ldots|ab\ldots}$ in this paper.

The Sobolev norm of functions f and g is defined as the square root of the Sobolev scalar product of the functions:

$$\|f,g\| = \sqrt{((f,g))} \quad . \tag{2}$$

Note that if the linear combination defining the Sobolev scalar product does not contain the Lebesgue scalar product of the zero derivatives of the functions, the Sobolev scalar product of a constant function with any function is zero. In this case, the Sobolev scalar product is not positive–definite, but only positive–semidefinite, and the Sobolev norm is not a norm, but only a seminorm. However, we may factorize the considered linear space of functions with respect to the space of functions keeping the Sobolev scalar product identically zero. In factor space, the Sobolev scalar product becomes positive–definite and the corresponding Sobolev seminorm becomes a norm. We will thus always speak of the “Sobolev norm”, even in the situations in which “Sobolev seminorm” would be more appropriate.

3 Sobolev norm in the objective function for inversion of seismic data

There are two main reasons for including the Sobolev norm in the inversion. Firstly, the Sobolev norm regularizes ill–conditioned inversions, which enables us to control the behaviour of the model functions in regions not illuminated by the data. The Sobolev norm is thus suitable for fitting discrete values with a velocity model. A typical example of such application is the fitting of structural interfaces for which the data are available only in some parts of the model. Secondly, the errors of many computational methods may be approximated by a function dependent on the corresponding Sobolev norm, which enables us to construct seismic models optimally smooth for the particular methods. For example, if we construct a model for full–wave finite differences, we may minimize the Sobolev norm approximating the propagation–velocity error due to the grid dispersion.

The Sobolev norm may, in general, be composed of the zero, first, second or higher derivatives of the functions describing the model. The model is very often described by cubic, bicubic or tricubic splines. Since the third homogeneous partial derivatives of the splines are discontinuous, the Sobolev scalar product composed of the fourth and higher derivatives could be infinite, and thus should be avoided. Simultaneously, minimization of the (zero derivatives of the) model functions usually has no meaning. We thus usually consider only Sobolev norms composed of the first, second and third derivatives. Since studies of the third derivatives have not yet been finished, we will concentrate on the first and second derivatives in this paper.

3.1 Fitting discrete values and regularizing an ill–conditioned inversion

Assume that we are fitting discrete values u^α at points $\mathbf{x}^\alpha$ inside the model volume by minimizing objective function

$$y = \sum_\alpha [\tilde{u}(\mathbf{x}^\alpha) - u^\alpha]^2 [\Delta u^\alpha]^{-2} + S^2 (\!(\tilde{u}, \tilde{u})\!) \quad , \tag{3}$$

where $\tilde{u}(\mathbf{x})$ is the model being constructed, Δu^α is the given standard deviation of value u^α given at point $\mathbf{x}{=}\mathbf{x}^\alpha$, and S is a manually chosen free parameter of the objective function which acts as a weighting factor of the Sobolev norm $(\!(\tilde{u}, \tilde{u})\!)$ of the model. For infinitely small weighting factor $S \to 0$, term $\sum_\alpha [\tilde{u}(\mathbf{x}^\alpha) - u^\alpha]^2 [\Delta u^\alpha]^{-2}$ in (3) is dominant, and the limit form

$$\tilde{\tilde{u}}(\mathbf{x}) = \lim_{S \to 0} \tilde{u}(\mathbf{x}) \tag{4}$$

of the solution corresponds (Klimeš 2000a) to the minimization of objective function

$$y = (\!(\tilde{\tilde{u}}, \tilde{\tilde{u}})\!) \tag{5}$$

with boundary conditions

$$\tilde{\tilde{u}}(\mathbf{x}^\alpha) = u^\alpha \quad . \tag{6}$$

For larger values of S, the influence of the minimization of the Sobolev norm increases, and the constructed model $\tilde{u}(\mathbf{x})$ fits the given values u^α only approximately.

The properties of interpolation between discrete values by means of minimizing the squares of different Sobolev norms has been investigated by Klimeš (2000a). He showed that the minimization of the first derivatives yields piecewise linear interpolation in 1-D. In 2-D and 3-D the interpolation tends to produce a constant function with singular spikes at given points $\mathbf{x}^\alpha$. The minimization of the second derivatives yields cubic splines in 1-D, in 2-D smooth interpolation with continuous first derivatives, and in 3-D smooth interpolation with continuous first derivatives between the given points, but with conical peaks at the given points. We can thus use the Sobolev norm composed of second derivatives for fitting discrete values.

Assume that we are fitting a structural interface with a smooth function. In such a case the data for the function are available only in that part of the model, where the interface is located. The behaviour of the function in other parts of the model is not given by the data, see, e.g., Figure 5. We might control the function by adding new artificial points to the data for the interface, but this manual intervention would probably slightly distort the modelled interface. It is much more convenient to control the function by increasing the weighting factor S of the Sobolev norm. A small increment of S will not influence the function in the region with the data, but will regularize its behaviour in the remaining parts of the model.

Another typical example of strongly ill–conditioned inversion is fitting a structural interface with an implicit function. Assume that the discrete points at the interface are given and that the interface cannot be fitted with an explicit function, e.g., such as $x_3 = w(x_1, x_2)$, but has to be described as the zero isosurface of function $f(x_1, x_2, x_3)$. We then minimize the deviations of function $f(x_1, x_2, x_3)$ from zero at the given points. Without additional a priori requirements, we would thus obtain an entirely zero function. One of the agreeable solutions is to fix the functional value at a specified point and to control the function in other than the given and the specified points by minimizing a suitable Sobolev norm. The specified point should be sufficiently distant from the interface. If the surface is closed, it may be located inside the block limited by the surface.

3.2 Constructing seismic models of optimal smoothness for a selected numerical method

The Sobolev norm is usually included in the inversion of seismic data if the numerical method to be applied to the model requires a smooth model. The Sobolev norm included in the objective function acts as a low–pass wavenumber filter (Klimeš 2000a).

We assume the objective function for the inversion of slowness or velocity $u(\mathbf{x})$ in the form of

$$y = \left[\int \mathrm{d}\mathbf{x}\right]^{-1} \int \mathrm{d}\mathbf{x}\, \tilde{C}(\mathbf{x},\mathbf{x}) + S^2 \|\tilde{u}\|^2 \quad , \tag{7}$$

where

$$\tilde{C}(\mathbf{x},\mathbf{x}') = < [\tilde{u}(\mathbf{x}) - u(\mathbf{x})][\tilde{u}(\mathbf{x}') - u(\mathbf{x}')] > \tag{8}$$

is the covariance function describing the deviation of model $\tilde{u}(\mathbf{x})$ from geological structure $u(\mathbf{x})$ (Klimeš 2002a), and S is the weighting factor of the Sobolev norm $\|\tilde{u}\|$ of the functions describing the model.

The first summand in (7) is the mean squared difference between the model and the geological structure. If possible, we choose the Sobolev norm $\|\tilde{u}\|$ so that $S\|\tilde{u}\|$ approximate the r.m.s. difference of the results of the numerical method under consideration from the exact solution in the model, expressed in units of $u(\mathbf{x})$. Objective function (7) then gains the clear physical meaning of the squared deviation of the model from the geological structure plus the squared deviation of the exact from the numerical results in the model. Note that by "exact solution" we mean the results, which we would obtain had we applied a hypothetical exact numerical method in the model.

For example, if the inaccuracy of the numerical method under consideration can be approximately characterized by the local relative travel–time standard deviation $\rho\tau_{\mathrm{method}}(\mathbf{x})$ describing the travel–time difference between the results of the numerical method under consideration from the exact results in the model, and, furthermore, if the square $[\rho\tau_{\mathrm{method}}(\mathbf{x})\ \tilde{u}(\mathbf{x})]^2$ of the deviation bilinearly depends on the derivatives of the interpolated parameter (slowness or velocity),

$$[\rho\tau_{\mathrm{method}}(\mathbf{x})\ \tilde{u}(\mathbf{x})]^2 \approx S^2\, b_{ij\ldots|ab\ldots}\ \tilde{u}_{,ij\ldots}(\mathbf{x})\ \tilde{u}_{,ab\ldots}(\mathbf{x}) \quad , \tag{9}$$

the Sobolev scalar product to be used in objective function (7) is defined by coefficients $b_{ij\ldots|ab\ldots}$ obtained from approximation (9):

$$\|\tilde{u}\|^2 = \left[\int\!\mathrm{d}\mathbf{x}\right]^{-1} \sum_{ij\ldots}\sum_{ab\ldots} \int\!\mathrm{d}\mathbf{x}\ b_{ij\ldots|ab\ldots}\ \tilde{u}_{,ij\ldots}(\mathbf{x})\ \tilde{u}_{,ab\ldots}(\mathbf{x}) \quad . \tag{10}$$

The selection of the Sobolev scalar products for particular numerical methods has been demonstrated by Klimeš (2000a) on examples of centred finite differences of the second order, network shortest–path ray tracing (Klimeš & Kvasnička 1994), 2-D first–order travel–time tracing (Podvin & Lecomte 1991), and 2-D second–order grid travel–time tracing (Klimeš 1996).

3.3 Constructing seismic models for ray tracing and Kirchhoff migrations

The feasibility and efficiency of ray tracing imposes relatively strong constraints on the smoothness of the velocity or slowness models. Unfortunately, we still have no quantitative criteria of applicability and accuracy of ray methods or their extensions. The situation is thus more complicated than in the case of the methods mentioned in Section 3.2. On the other hand, the numerical efficiency of ray tracing can be evaluated in terms of the "average Lyapunov exponent", introduced by Klimeš (2000c, 2002b) for 2-D models without structural interfaces.

In complex models, the behaviour of rays becomes chaotic and the geometrical spreading, number of arrivals and density of caustic surfaces increase exponentially with travel time. The exponential increment may be quantitatively described in terms of the "average Lyapunov exponent" for the model. The "average Lyapunov exponent" may roughly be approximated by the square root of the Sobolev norm composed of the second partial derivatives of the functions describing the slowness or velocity field in the model (Klimeš 2000a). This enables us to determine the quantitative criteria on models, so as to be suitable for ray tracing, in terms of Sobolev scalar products. We choose the maximum "average Lyapunov exponent" for the model, we estimate the maximum Sobolev norm of the model, and we estimate the value of weighting factor S. We then perform the inversion, compute the values of the "average Lyapunov exponent" and the Sobolev norm in the inverted model, re-estimate the value of S, and continue iteratively with the inversion until we obtain the model of the required smoothness. We may thus construct models in which ray tracing will be possible and numerically efficient. We remind the reader, that we know nothing about the applicability and accuracy of ray tracing in the models.

For example, to construct a model suitable for ray–based migrations, Klimeš (2000b) chose the value of the "average Lyapunov exponent" $\bar{\lambda}$ for the model as

$$\bar{\lambda} \leq \frac{2}{T_{\max}} \quad , \tag{11}$$

where $T_{\max} \geq T_S + T_R$ is the maximum sum of travel times from the source and from the receiver. The product of the average numbers of arrivals from a source and a receiver then probably does not exceed 1.8, and the product of maximum numbers of arrivals from a source and a receiver then probably does not exceed 7.

If we choose coefficients

$$b_{ij|ab} = \frac{1}{3}\left(\delta_{ij}\,\delta_{ab} + \delta_{ia}\,\delta_{jb} + \delta_{ib}\,\delta_{ja}\right) \tag{12}$$

of the Sobolev norm according to Klimeš (2000b), the Sobolev norm $\|u\|$ of the model satisfying equation (11) should obey equation (Klimeš 2000b)

$$\|u\| \leq \sqrt{\frac{8}{3}}\left[\frac{4 + 2\,K_{\mathrm{osc}}\ln 2}{T_{\max}}\right]^2 \frac{1}{\langle v\rangle^3} \quad , \tag{13}$$

where $\langle v\rangle$ is the average velocity in the model, and K_{osc} is the average number of velocity oscillations (i.e. the average number of focusing and defocusing velocity zones) along rays of length corresponding to $T_{\max}$. δ_{ij} in equation (12) is the Kronecker delta.

4 Numerical examples

Routines for application of the above described minimization of the Sobolev norm during the seismic inversion have been coded and incorporated into existing Fortran 77 package `MODEL`, which serves to specify heterogeneous seismic models composed of smooth blocks with arbitrary varying seismic parameters. For the description of the basic ideas of the model specification refer to Červený *et al.* (1988), the latest version of the package may be found at http://seis.karlov.mff.cuni.cz/consort/main.htm . Package `CRT`, available at the same place, is used for ray tracing in the models. All the computations are carried out on a PC Pentium with 64 Mbytes of memory.

The memory requirements of the current coding of the method are $M(D + M)$ storage locations, where M is the number of model parameters, and D is the number of data points. The requirements create no problems for 2-D model Hess, but they disallow the use of all the data and achieving the minimum error in inversion of the 3-D SEG/EAGE Salt Model and of 2-D model Pluto 1.5.

Smoothing 2-D model Hess is an example of smoothing a given rough model by generating the values in the rough model and fitting them with the smooth model. In the case of the SEG/EAGE 3-D Salt Model, only gridded velocities and triangulated interfaces are given. From the point of view of ray tracing, the gridded velocities and the points at the interfaces are not a model, because for ray tracing the values of material parameters must be known at each point of the model volume. Building the SEG/EAGE 3-D Salt Model is thus an example of constructing a 3-D model by inversion of given data. In the case of 2-D model Pluto 1.5, only gridded velocities are given, but the model contains three salt bodies. The data for construction of structural interfaces thus must be taken from the velocity grid.

For another example of using the Sobolev norms to construct velocity models, refer to Žáček (2002).

4.1 Smoothing 2-D model Hess for Kirchhoff migrations

4.1.1 Data and model parametrization

2-D model Hess is specified in the form of a file with input data for the `MODEL` package. The dimensions of the model are 40200 times 21000 feet. Two interfaces in the model, limiting a salt body, are parametrized by B–splines with 64 spline points spaced at 200 feet. Background velocities are parametrized by B–splines with 202×106 spline points with a spacing of $200\,\mathrm{ft} \times 200\,\mathrm{ft}$; the velocity inside the salt body is constant. See Figure 1.

We perform several tests of ray tracing in the original model. The behaviour of the ray field seems to be too complicated with too many caustics, especially in the low velocity channel near the surface of the model, see Figures 2 to 4. We thus decide to smooth the model by means of inversion of the values at the spline points with minimization of the Sobolev norms of the model.

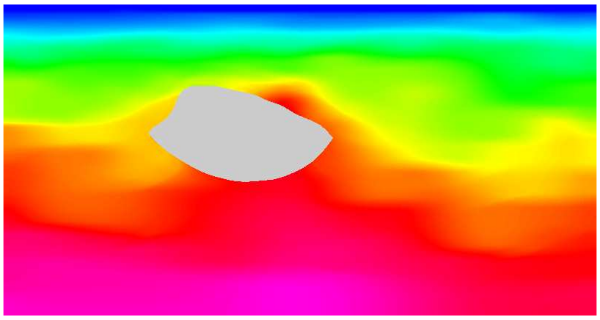

Figure 1: P-wave velocity in the original model (before smoothing). The background velocity varies from $5000\,\mathrm{ft\,s^{-1}}$ at the top of the model to $9800\,\mathrm{ft\,s^{-1}}$ at the bottom. The velocity of the salt body is constant and equals $14800\,\mathrm{ft\,s^{-1}}$. The horizontal dimension of the model is 40200 ft, its vertical dimension is 21000 ft.

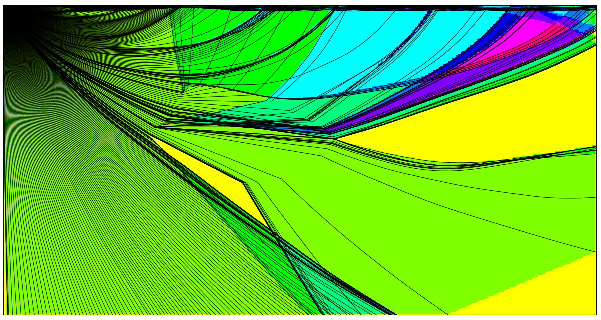

Figure 2: The numbers of travel times and the rays computed for the refracted wave in the original model. The point source is located in the top left corner of the model. The yellow colour corresponds to no travel time, green to 2 arrivals, cyan to 4, blue to 6, magenta to 8, red to 10 arrivals. The extents of the figure are the same as of Fig. 1.

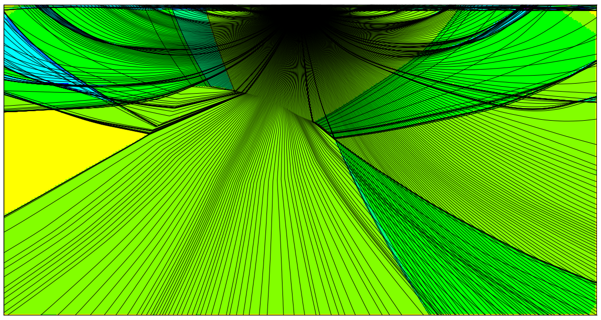

Figure 3: The numbers of travel times and the rays computed for the source located in the middle of the top of the model. The colour scale is the same as in Fig. 2. The extents of the figure are the same as of Fig. 1.

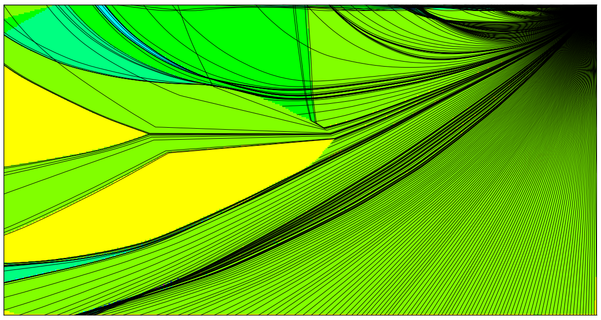

Figure 4: The numbers of travel times and the rays computed for the source located in the top right corner of the model. The colour scale is the same as in Fig. 2. The extents of the figure are the same as of Fig. 1.

In Figure 1, we can see that the horizontal variation of the velocity field is less pronounced than the vertical variation, and that the vertical variation is greater in the shallow parts of the model than in its deeper parts. The interfaces are quite smooth, but the edges are sharp. According to these observations, we manually choose a new parametrization of the model. Let us emphasize that the parametrization is based on the author's opinion, and is expected to be optimized during the inversion. The parametrization is as follows: for the interfaces we take an irregular B–spline grid of 28 points with 26 points regularly spaced at 500 feet in the region of the salt body and 2 points at the sides of the model. The two points enable us to control the behaviour of the functions describing the interfaces in the parts of model not covered by the data for the interfaces. For the background velocity, we take a horizontally regular grid of 17 points spaced at 2500 feet and a vertically irregular grid of 31 points spaced at 200 feet at the top to 800 feet at the bottom.

4.1.2 Choosing the maximum Lyapunov exponent

To estimate the maximum sum of travel times from a source and a receiver, we compute the average slowness of the model $\langle u \rangle = 0.120611\ 10^{-3}\,\mathrm{s\,ft}^{-1}$. If we consider the maximum sum of the ray paths to be about 50000 feet, we arrive at the estimation that the maximum sum of travel times from a source and a receiver is limited by $T_{\max} = 6\,\mathrm{s}$. According to equation (11), we choose the maximum "average Lyapunov exponent" $\bar{\lambda}_{\max}$ of the new model as

$$\bar{\lambda}_{\max} = \frac{2}{T_{\max}} = 0.333\,\mathrm{s}^{-1} \quad . \tag{14}$$

4.1.3 Choosing the maximum Sobolev norm of the model

Analogously to equation (13) we choose the maximum Sobolev norm $\|v\|_{\max}$ of the velocity field in the new model as

$$\|v\|_{\max} = \sqrt{\frac{8}{3}} \left[\frac{4 + 2\,K_{\mathrm{osc}} \ln 2}{T_{\max}} \right]^2 \frac{1}{\langle v \rangle} = 2.6\ 10^{-4}\,(\mathrm{ft\,s})^{-1} \quad , \tag{15}$$

where $\langle v \rangle = 8074.73\,\mathrm{ft\,s}^{-1}$ is the average velocity of the background, and the average number K_{osc} of focusing and defocusing zones is roughly estimated to be 3 for the rays which pass the salt, and to be 1 for the other rays; we thus calculate with $K_{\mathrm{osc}} = 2$.

In this example, we first try to apply the minimum reasonable smoothing of the interfaces. We thus do not prescribe the maximum Sobolev norm of the interfaces.

4.1.4 Inversion and smoothing

The objective function is taken in the form

$$y = \left(\frac{|x - x_0|}{\sigma_x} \right)^2 + (S_x \|x\|)^2 + \left(\frac{|v - v_0|}{\sigma_v} \right)^2 + (S_v \|v\|)^2 \quad , \tag{16}$$

where $|x - x_0|$ is the standard deviation of the position of the interfaces in the smooth model from the gridded interfaces in the original model, $\|x\|$ is the 2-D Sobolev norm of the curvature of the interfaces in the smoothed model, $|v - v_0|$ is the standard velocity deviation of the model from the original gridded velocities, and $\|v\|$ is the 2-D Sobolev norm of the velocity field in the smoothed model. S_x and S_v are numerical parameters which control the smoothing during the inversion. We use unit given velocity deviation $\sigma_v = 1\,\mathrm{ft\,s}^{-1}$ and unit given interface deviation $\sigma_x = 1\,\mathrm{ft}$ in the selected objective function.

The inversion of the interfaces and the inversion of the velocity field are mutually independent in this example. We can thus perform the inversion of the interfaces in the first step, and the inversion of the velocity in the second step.

4.1.4.1 Inversion of the interfaces

We choose $S_v = 0\,\mathrm{ft\,s}$, and perform the inversion without smoothing of the velocity, which we are not interested in at the moment.

In this example, we try to apply the minimum reasonable smoothing of the interfaces. We thus start the inversion without smoothing of the interfaces, with $S_x = 0\,\mathrm{ft}$ (the interfaces are smoothed just by the projection onto the B–splines). We obtain oscillations of both surfaces, which produce a salt body other than that given by the data, see Figure 5. In the next steps of inversion we thus include the minimization of the curvature of the interfaces by increasing the value of S_x. When we reach approximately the value of $S_x = 2500\,\mathrm{ft}$, the spurious salt body moves outside the model volume. We thus consider the value of $S_x = 2500\,\mathrm{ft}$ as the value corresponding to the minimum reasonable smoothing of the interfaces. Whether the interfaces are sufficiently smooth will be tested by ray tracing.

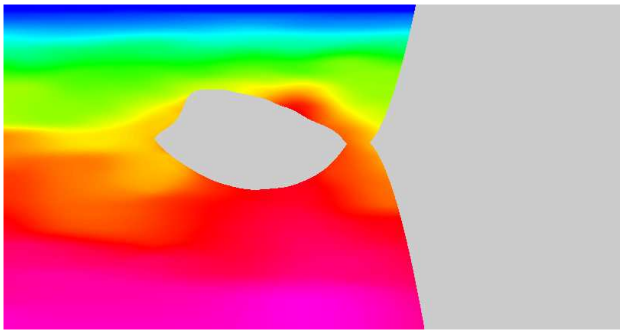

Figure 5: Inversion of the interfaces without the Sobolev norm. The oscillations of the surfaces limiting the lenticular salt body produced another spurious salt body on the right–hand side of the model. The colour scale and the extents of the figure are the same as of Fig. 1.

We compute standard interfaces deviation $|x - x_0| = 5.6\,\mathrm{ft}$. This deviation causes a travel–time error of approximately

$$dT = |x - x_0| \left| \frac{1}{\langle v \rangle} - \frac{1}{v_{\mathrm{salt}}} \right| = 3.15\ 10^{-4}\,\mathrm{s} \quad , \tag{17}$$

where $\langle v \rangle = 8074.73\,\mathrm{ft\,s^{-1}}$ is the average velocity of the background and $v_{\mathrm{salt}} = 14800\,\mathrm{ft\,s^{-1}}$ is the velocity of the salt.

4.1.4.2 Inversion of the velocity field

We have selected the value of $S_x = 2500\,\mathrm{ft}$, which ensures the proper position of the interfaces. We will retain this value during the velocity inversion.

(a) First iteration

We first perform the inversion with $S_v = 0\,\mathrm{ft\,s}$ (i.e. without smoothing), and obtain the standard velocity deviation of the model

$$|v - v_0| = 13.94\,\mathrm{ft\,s^{-1}} \quad . \tag{18}$$

The Sobolev norm of the velocity field smoothed just by the projection onto the B–splines

$$\|v\| = 37.\ 10^{-4}\,(\mathrm{ft\,s})^{-1} \quad , \tag{19}$$

is large, see equation (15).

(b) Second iteration

We choose

$$S_v = \frac{|v - v_0|}{\sigma_v \|v\|_{\max}} \quad , \tag{20}$$

as in the paper by Klimeš (2000b, eq. 20). Then

$$S_v = \frac{13.94}{2.6\ 10^{-4}} \,\mathrm{ft\,s} = 53615 \,\mathrm{ft\,s} \quad , \tag{21}$$

and we enter the rounded value of

$$S_v = 50000 \,\mathrm{ft\,s} \tag{22}$$

for the second iteration. The resulting Sobolev norm

$$\|v\| = 2.9\ 10^{-4} \,(\mathrm{ft\,s})^{-1} \tag{23}$$

of the velocity looks acceptable, see equation (15).

(c) Subsequent iterations

The presence of the structural interfaces and the existence of the low velocity channel at the top of the model have not been taken into account during the estimation of S_v. We thus choose several values of S_v for subsequent iterations in order to see the behaviour of the model in dependence on S_v. After each inversion we perform several tests. For each model we compute the standard velocity deviation from the velocity in the original model, the value of "average Lyapunov exponent" $\bar{\lambda}$ and the maximum number of arrivals $N_{\max}$ from the source located in the left top corner of the model. The results of the computations are in Table 1.

	$\|v - v_0\|/(\mathrm{ft\,s^{-1}})$	$\\|v\\|/((\mathrm{ft\,s})^{-1})$	$\bar{\lambda}/(\mathrm{s^{-1}})$	$N_{\max}$
desired values		$2.6\ 10^{-4}$	0.333	
original model			0.423	11
$S_v = 0 \,\mathrm{ft\,s}$	13.94	$37.0\ 10^{-4}$	0.380	7
$S_v = 17500 \,\mathrm{ft\,s}$	15.19	$4.9\ 10^{-4}$	0.345	6
$S_v = 35000 \,\mathrm{ft\,s}$	17.41	$3.5\ 10^{-4}$	0.316	5
$S_v = 50000 \,\mathrm{ft\,s}$	19.24	$2.9\ 10^{-4}$	0.300	5
$S_v = 70000 \,\mathrm{ft\,s}$	21.42	$2.4\ 10^{-4}$	0.287	5

Table 1: Results of the inversion of the velocity field in model Hess in dependence on weighting factor S_v of the Sobolev norm used.

We can see that for $S_v = 0 \,\mathrm{ft\,s}$ we obtain a standard velocity deviation of about $14 \,\mathrm{ft\,s^{-1}}$. The desired value of $\bar{\lambda} = 0.333 \,\mathrm{s^{-1}}$ corresponds to a velocity deviation of about $16 \,\mathrm{ft\,s^{-1}}$. Most of the velocity deviation is thus caused by the projection onto the B–splines, and we should try the inversion with a finer parametrization of the model.

A figure of the Fourier spectrum of the velocity deviation should help us to decide, in which direction and how many times we should densify the parametrization of the model. We must keep in mind that the parametrization must not be denser than the data.

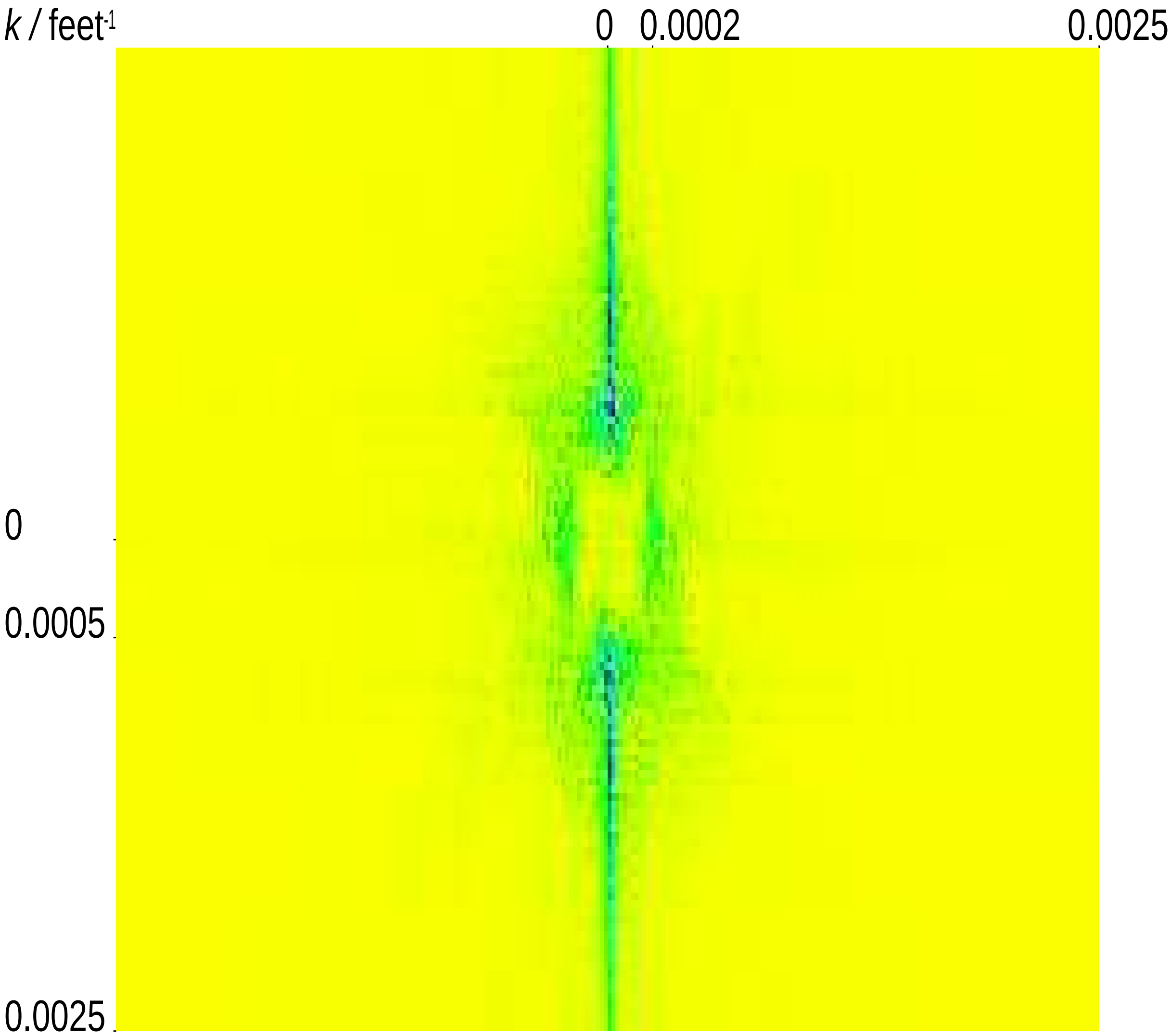

Figure 6: Fourier spectrum of the velocity deviation of the smoothed model obtained with $S_v = 50000\,\mathrm{ft\,s}$. The extents of the figure correspond to wavenumbers k from $-0.0025\,\mathrm{ft}^{-1}$ to $0.0025\,\mathrm{ft}^{-1}$. The light rectangle in the middle of the figure shows the wavenumbers k of the velocity field which the model fits. We can see that the model fits the velocity variations of wavelength greater than approximately 2500 ft horizontally and 1000 ft vertically.

4.1.5 Finer B–spline parametrization of the model

We choose the new parametrization of the model as follows: for the interfaces we retain the irregular B–spline grid of 28 points; for the background velocity we take a horizontally regular grid of 26 points spaced at 1600 feet and a vertically irregular grid of 58 points spaced at 200 to 400 feet.

We now have $56+1+26\times 58 = 1565$ B–spline points, and the memory requirements of the inversion are 36180865 storage locations. This is too much for our computer and we thus cannot use all the data. We resample the data in the horizontal direction and use a data grid of 67 points spaced at 600 feet horizontally and the original 106 points spaced at 200 feet vertically.

Note that, with the new parametrization, we are not able to perform the inversion with $S_v = 0\,\mathrm{ft\,s}$, because we now have more background velocity B–spline gridpoints in the salt body, and the inversion becomes ill-conditioned. We performed several tests of

	$\lvert v - v_0 \rvert / (\mathrm{ft\,s^{-1}})$	$\lVert v \rVert / ((\mathrm{ft\,s})^{-1})$	$\lambda / (\mathrm{s^{-1}})$	$N_{\max}$
desired values		$2.6\ 10^{-4}$	0.333	
original model			0.423	11
$S_v = 1000\,\mathrm{ft\,s}$	5.52	$12.3\ 10^{-4}$	0.398	6
$S_v = 10000\,\mathrm{ft\,s}$	7.28	$6.5\ 10^{-4}$	0.365	5
$S_v = 17500\,\mathrm{ft\,s}$	9.03	$5.2\ 10^{-4}$	0.343	5
$S_v = 25000\,\mathrm{ft\,s}$	10.68	$4.4\ 10^{-4}$	0.327	5
$S_v = 35000\,\mathrm{ft\,s}$	12.75	$3.7\ 10^{-4}$	0.313	5

Table 2: Results of the inversion of the velocity field in model Hess with finer B–spline parametrization of the model.

S_v with the new parametrization of the model, see Table 2.

We see that the standard velocity deviation caused by the projection onto the B–splines is now much smaller than for the previous model parametrization, and that the deviation increases as we increase S_v in order to meet the requirements imposed on the model smoothness.

4.1.6 Numerical tests of the smoothed model

The model with the finer parametrization obtained after the inversion with values of $S_x = 2500\,\mathrm{ft}$ and $S_v = 25000\,\mathrm{ft\,s}$ has been selected as the best model.

The standard relative velocity deviation from the velocity in the original model is 0.18 %. The standard deviation of the interfaces is 5.6 ft.

For the gridded P-wave velocity in the model, the gridded velocity deviation, the Fourier spectrum of the gridded velocity deviation, and the tests of ray tracing of a refracted wave, see Figures 7 to 12.

4.2 Building the SEG/EAGE 3-D Salt Model for Kirchhoff migrations

4.2.1 Data for the model

The SEG/EAGE 3-D Salt Model (Aminzadeh *et al.* 1997) is specified in the form suitable for the `GOCAD` modelling software. The dimensions of the model are 13500 times 13500 times 4200 metres. Several interfaces in the model are stored in the form of triangulated surfaces, and the 3-D velocity cube is given. From the point of view of ray tracing, the gridded velocities and the points at the interfaces are not a model, because the values of the material parameters must be known at each point of the model volume for ray tracing. This example is thus principally different from the example of smoothing of the Hess model. On the other hand, the process of building of the Salt model is technically the same as the process of smoothing of the Hess model. We take the data and build a 3-D model by inversion. In the first example, we shall construct a smooth model without interfaces, and in the second example a model containing the salt body and some other selected interfaces.

The P-wave velocity is discretized on a grid of $676 \times 676 \times 210$ points with a spacing of $20 \times 20 \times 20\,\mathrm{m}$. This is a very large amount of data, and we immediately see that a much sparser grid must be used for the data for the inversion. We thus resample the velocities to the grid with the spacing $40 \times 40 \times 40\,\mathrm{m}$, which fits into the 64 Mbytes of available memory. On this grid we convert the velocity into the slowness. On the slowness grid we perform arithmetic averaging and we calculate slownesses on

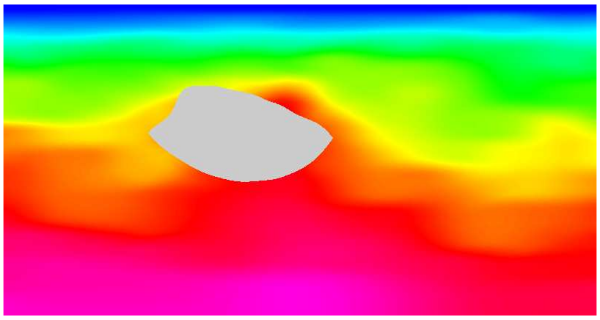

Figure 7: P-wave velocity in the smoothed model. The background velocity varies from $5000\,\mathrm{ft\,s^{-1}}$ at the top of the model to $9800\,\mathrm{ft\,s^{-1}}$ at the bottom. The velocity of the salt body is constant and equals $14800\,\mathrm{ft\,s^{-1}}$. The horizontal dimension of the model is 40200 ft, its vertical dimension is 21000 ft.

Figure 8: Deviation of the gridded velocity in the smoothed model from the gridded velocity in the original model. The yellow colour corresponds to zero deviation, red to negative and green to positive deviation. The maximum velocity deviation is $103.1\,\mathrm{ft\,s^{-1}}$. The standard velocity deviation is $10.68\,\mathrm{ft\,s^{-1}}$, the standard relative velocity deviation is 0.18 %.

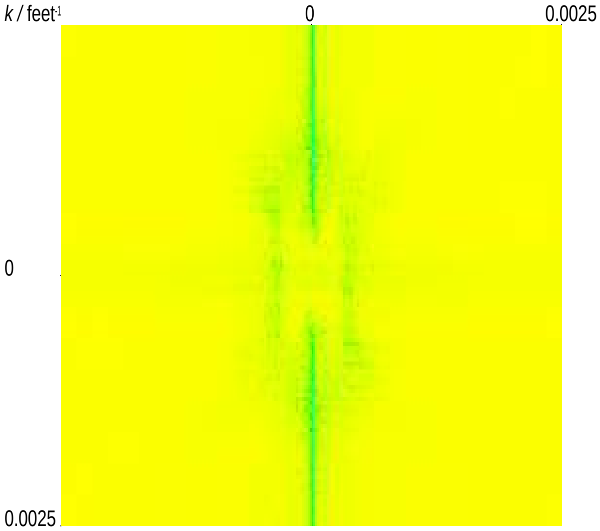

Figure 9: Fourier spectrum of the velocity deviation from Figure 8. The extents of the figure correspond to wavenumbers k from $-0.0025\,\mathrm{ft^{-1}}$ to $0.0025\,\mathrm{ft^{-1}}$.

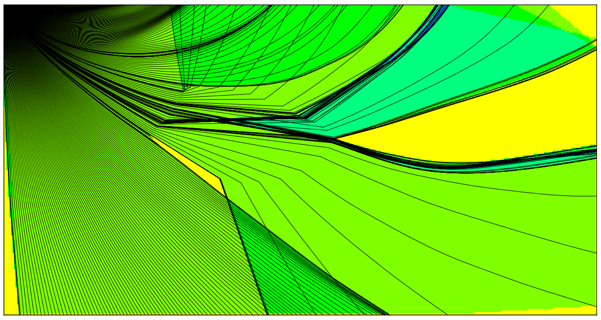

Figure 10: The numbers of travel times and the rays computed for the refracted wave in the smoothed model. The source is located in the left top corner of the model. The colour scale is the same as in Fig. 2.

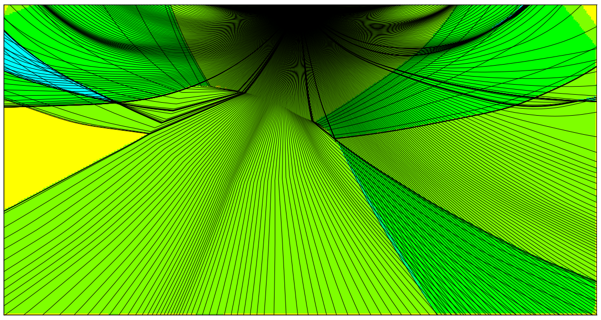

Figure 11: The numbers of travel times and the rays computed in the smoothed model for the source located in the middle of the top of the model. The colour scale is the same as in Fig. 2.

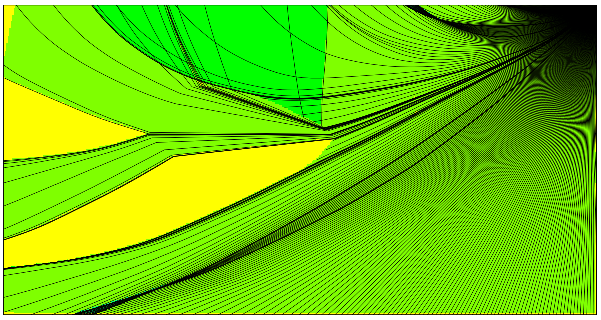

Figure 12: The numbers of travel times and the rays computed in the smoothed model for the source located in the top right corner of the model. The colour scale is the same as in Fig. 2.

the individual sparser grids of different dimensions which are then used as the data for the inversion. We have decided to average the slownesses as the data for the inversion rather than the velocities, because the averaging of the slownesses preserves the ray travel times.

4.2.2 The grid for the calculation of the velocity and slowness deviations and the model spline grids

The calculation of velocity deviations on the full $20 \times 20 \times 20\,\mathrm{m}$ grid is very time consuming. We thus looked for a sparser grid, which would speed up the calculation, providing approximately the same results as the full grid. We decided to use the grid with the spacing $60 \times 60 \times 20\,\mathrm{m}$ for the calculation of the deviations.

The structural interfaces in the models and the 3-D velocity fields are modelled by tricubic B–splines, which are defined by the values specified at the gridpoints of the model spline grids. The number of model parameters thus corresponds to the dimensions of the model spline grids. Due to the limited computer memory, the dimensions of the model spline grids must be chosen carefully.

4.2.3 Choosing the maximum Lyapunov exponent and the maximum Sobolev norm

To estimate the maximum sum of travel times from a source and a receiver, we compute the average slowness of the model $\langle u \rangle = 0.428\ 10^{-3}\,\mathrm{s\,m^{-1}}$. If we consider the maximum sum of the ray paths to be about 14500 m, we arrive at the estimation that the maximum sum of the travel times from a source and a receiver is limited by $T_{\mathrm{max}} = 6.21\,\mathrm{s}$. Analogously as for model Hess we choose the maximum "average Lyapunov exponent" $\bar{\lambda}_{\mathrm{max}}$ of the model as

$$\bar{\lambda}_{\mathrm{max}} = \frac{2}{T_{\mathrm{max}}} = 0.322\,\mathrm{s}^{-1} \quad . \tag{24}$$

The maximum Sobolev norm $\|u\|_{\mathrm{max}}$ of the slowness field in the model chosen according to equation (13) is

$$\|u\|_{\mathrm{max}} = \sqrt{\frac{8}{3}} \left[\frac{4 + 2\,K_{\mathrm{osc}} \ln 2}{T_{\mathrm{max}}} \right]^2 \frac{1}{\langle v \rangle^3} = 0.152\ 10^{-9}\,\mathrm{s\,m^{-3}} \quad , \tag{25}$$

where $\langle v \rangle = 2336.44\,\mathrm{m\,s^{-1}}$ is the average velocity in the model, and average number K_{osc} of focusing and defocusing zones is estimated as $K_{\mathrm{osc}} = 2$.

Again, as in model Hess, we have no quantitative criteria on the smoothness of the structural interfaces, and we thus first try to apply the minimum reasonable smoothing of the interfaces. Whether the interfaces are sufficiently smooth will be tested by ray tracing.

4.2.4 Smooth version of the Salt Model

We try to fit the data by a smooth model, composed of one block with three–dimensionally varying velocity. The data for the inversion are the slownesses on a coarser grid, as mentioned above. In the model, we are interpolating the slowness by tricubic B-splines. The inversion is linear, with objective function

$$y = \left(\frac{|u - u_0|}{\sigma_u} \right)^2 + (S_u \|u\|)^2 \quad , \tag{26}$$

where $|u-u_0|$ is the standard slowness deviation of the model from the gridded slownesses, $\|u\|$ is the 3-D Sobolev norm of the slowness field in the model, and $\sigma_u = 1\,\mathrm{s\,m^{-1}}$ is the given unit slowness deviation.

We first perform the inversion with $S_u = 0\,\mathrm{m^3\,s^{-1}}$ and search for the best model parametrization, which would yield the lowest standard relative velocity deviation $|\frac{v-v_0}{v_0}|$ of the velocity in the model from the velocity in the data cube. We start with slowness data grid intervals of $500 \times 500 \times 500$ m and model B-spline intervals of $1000 \times 1000 \times 1000$ m. We then try denser and sparser spline grids. We find that the spline grid should be densified vertically, and that the data grid may be sparser horizontally, see Table 3.

$\frac{\text{number of data gridpoints}}{\text{data grid intervals/ m}}$	$\frac{\text{number of model spline points}}{\text{model spline intervals/ m}}$	$\lvert\frac{v-v_0}{v_0}\rvert/(\%)$	$\|u\|/(\mathrm{s\,m^{-3}})$	$\bar{\lambda}/(\mathrm{s^{-1}})$
$\frac{28\times28\times9}{500\times500\times500}$	$\frac{15\times15\times5}{1000\times1000\times1000}$	9.50	$0.172\ 10^{-9}$	0.260
$\frac{28\times28\times9}{500\times500\times500}$	$\frac{9\times15\times5}{1750\times1000\times1000}$	9.68	$0.155\ 10^{-9}$	0.250
$\frac{28\times28\times9}{500\times500\times500}$	$\frac{24\times15\times5}{600\times1000\times1000}$	9.47	$0.185\ 10^{-9}$	0.264
$\frac{28\times28\times9}{500\times500\times500}$	$\frac{15\times15\times8}{1000\times1000\times500}$	7.80	$0.378\ 10^{-9}$	0.298
$\frac{23\times23\times11}{600\times600\times400}$	$\frac{15\times15\times5}{1000\times1000\times1000}$	9.48	$0.174\ 10^{-9}$	0.262
$\frac{23\times23\times11}{600\times600\times400}$	$\frac{15\times15\times9}{1000\times1000\times500}$	7.63	$0.480\ 10^{-9}$	0.362
$\frac{18\times18\times17}{800\times800\times250}$	$\frac{15\times15\times9}{1000\times1000\times500}$	7.54	$0.511\ 10^{-9}$	0.374
$\frac{18\times18\times17}{800\times800\times250}$	$\frac{12\times12\times14}{1200\times1200\times300}$	7.13	$0.833\ 10^{-9}$	0.441
$\frac{14\times14\times21}{1000\times1000\times200}$	$\frac{12\times12\times14}{1500\times1500\times250}$	7.29	$1.086\ 10^{-9}$	0.516
desired values			$0.152\ 10^{-9}$	0.322

Table 3: Results of the inversion of the velocity field in the Salt Model without smoothing.

For the best model parametrization $\frac{12\times12\times14}{1200\times1200\times300}$ and the data $\frac{18\times18\times17}{800\times800\times250}$ we calculate the standard slowness deviation $|u-u_0| = 0.322\ 10^{-4}\,\mathrm{s\,m^{-1}}$, we estimate

$$S_u = \frac{|u-u_0|}{\sigma_u \|u\|_{\max}} = \frac{0.322\ 10^{-4}\,\mathrm{s\,m^{-1}}}{1\,\mathrm{s\,m^{-1}}\ 0.152\ 10^{-9}\,\mathrm{s\,m^{-3}}} = 211842\,\mathrm{m^3\,s^{-1}} \quad , \tag{27}$$

as in model Hess, and we enter the rounded value of

$$S_u = 200000\,\mathrm{m^3\,s^{-1}} \quad , \tag{28}$$

for the second iteration. We then choose several values of S_u in order to see how the model behaves in dependence on S_u, see Table 4.

	$\lvert\frac{v-v_0}{v_0}\rvert/(\%)$	$\|u\|/(\mathrm{s\,m^{-3}})$	$\lambda/(\mathrm{s^{-1}})$
$S_u = 0\,\mathrm{m^3\,s^{-1}}$	7.13	$0.833\ 10^{-9}$	0.441
$S_u = 25000\,\mathrm{m^3\,s^{-1}}$	7.64	$0.400\ 10^{-9}$	0.340
$S_u = 50000\,\mathrm{m^3\,s^{-1}}$	8.22	$0.254\ 10^{-9}$	0.308
$S_u = 100000\,\mathrm{m^3\,s^{-1}}$	9.02	$0.153\ 10^{-9}$	0.263
$S_u = 200000\,\mathrm{m^3\,s^{-1}}$	9.85	$0.091\ 10^{-9}$	0.224
desired values		$0.152\ 10^{-9}$	0.322

Table 4: Results of the inversion of the velocity field in the Salt Model in dependence on weighting factor S_u of the Sobolev norm used.

We consider the model obtained after the inversion with the value of $S_u = 50000\,\mathrm{m^3\,s^{-1}}$ as the best smooth model, which meets our requirements.

4.2.5 Salt Model - version with interfaces

We try to fit the data by a model containing the most important interfaces, which are characterized by the highest discontinuities in the velocity field. These interfaces are the ocean bottom, the interface limiting the salt body, the geopressure horizon, and the bottom flat interface. Concerning the velocity field, we use the slownesses on the coarser grid as the data, and we interpolate the slowness by tricubic B-splines in the model. The inversion is again linear with objective function

$$y = \left(\frac{|x - x_0|}{\sigma_x}\right)^2 + (S_x\|x\|)^2 + \left(\frac{|u - u_0|}{\sigma_u}\right)^2 + (S_u\|u\|)^2 \quad . \tag{29}$$

The inversion of the interfaces and the inversion of the velocity field are again mutually independent, as in model Hess. We can thus perform the inversion of the interfaces in the first step, and the inversion of the velocity in the second step. This fact is of great importance, because to invert the velocity we must know the block of the model, in which the gridpoint is located, for each data gridpoint. This information may be computed after inverting the interfaces, and we are then able to invert the velocities.

4.2.5.1 Inversion of the interfaces

For all the interfaces, except the salt interface, we may use the triangulated surfaces in the `GOCAD` representation as the data for inversion. In case of the salt interface, the corresponding `GOCAD` file contains all the triangles of the interface. We tried to model the interface by one surface, but all our attempts failed, and the salt interface must be fitted by two surfaces. We thus generate two files according to the discontinuity in the velocity cube corresponding to the surface of the salt body: one file with the points at the top of the salt, and one with the points at the bottom of the salt. We have now 4 data points for the top of the model, 601 data points for the ocean bottom, 1780 points for the geopressure horizon, 4 points for the bottom, 6425 points for the salt top, and 6336 data points for the salt bottom.

We choose the starting parametrization of the interfaces manually, as in model Hess. We first invert the interfaces with $S_x = 0\,\mathrm{m}$, and then increase the value of S_x until we reach the minimum reasonable smoothing of the interfaces, characterized by acceptable values of standard interface deviations. We also optimize the B-spline grids for the interfaces. Finally, the top of the model and the bottom interface are modelled by constant functions, the ocean bottom is parametrized by 6 times 6 spline points spaced at 2800 metres, the geopressure horizon is parametrized by 8 times 8 points spaced at 2000 metres, both the top and the bottom of the salt are parametrized by 20 times 21 points spaced at 400 metres. Note, that we have enough data to densify the parametrization of the geopressure horizon and of the salt interfaces, but this is not possible due to the limited computer memory.

Another possibility for the inversion of the interfaces is to split the `GOCAD` file with the salt interface into two files, one with 990 points for the top of the salt, and the second with 577 points for the bottom of the salt. We may now densify the parametrization of the geopressure horizon to 29 times 29 points spaced at 500 metres, the parametrization of the salt bottom may be densified to 24 times 23 points spaced at 350 metres, and the parametrization of the salt top may be densified to 32 times 31 points spaced at 250 metres. The root mean square of the error in the position of the geopressure horizon then decreases from 72 m to 9 m, from 63 m to 43 m for the salt top, and from 31 m to 23 m for the salt bottom, but the standard relative deviation of the velocity field in the model increases compared to the model obtained by inversion of the data points at interfaces obtained from the velocity cube, see Table 5. This fact is not fully understood by the author.

	$\frac{\|u\|}{(\mathrm{s\,m^{-3}\,10^{-9}})}$	$\frac{\|\frac{v-v_0}{v_0}\|}{(\%)}$	$\frac{\|\frac{u-u_0}{u_0}\|}{(\%)}$	$\frac{\|v-v_0\|}{(\mathrm{m\,s^{-1}})}$	$\frac{\|u-u_0\|}{(\mathrm{s\,m^{-1}\,10^{-4}})}$
data from velocity field	0.199	5.53	5.86	143	0.208
data from GOCAD files	0.199	6.64	6.62	168	0.229
data from GOCAD files, gp2 densified	0.199	6.57	6.57	167	0.226
data from GOCAD files, salt densified	0.199	6.34	6.52	162	0.224

Table 5: Results of the inversion in the Salt Model in dependence on the data used for the salt interface and in dependence on the parameterization of the geopressure horizon and of the salt surfaces. Velocity is described by the same functions in all the four models.

4.2.5.2 Inversion of the velocity field

The first test is analogous to the velocity inversion in the smooth model. As the data, we again use slownesses computed by arithmetical averaging. We start the velocity inversion with the value $S_u = 0\,\mathrm{m^3\,s^{-1}}$ and a manually selected parametrization of the velocity field, and we search for the best combination of data grid and B-spline grids for the velocity outside the salt body. We then include the smoothing of the velocity field and we examine the behaviour of the model in dependence on S_u. Due to the limited computer memory, we must use as sparse data grid as possible, in order to be able to densify the model parametrization. On the other hand, the data grid must be always denser than the model parametrization.

We start with the data grid of $68 \times 68 \times 20$ points spaced at $200 \times 200 \times 200\,\mathrm{m}$. Table 6 demonstrates, that the data may be sparser horizontally, but should be densified vertically. The results also show, that the error decreases when we increase the weight S_u from $0\,\mathrm{m^3\,s^{-1}}$ up to the values about $25000\,\mathrm{m^3\,s^{-1}}$. This fact is not understood by the author.

Another test have been done with the slownesses used as the data for the velocity inversion in the model parametrized by $5\times5\times3$ points spaced at $3500\times3500\times \sim 1700\,\mathrm{m}$. Four kinds of the data have been prepared on the grid of $68 \times 68 \times 20$ points spaced at $200 \times 200 \times 200\,\mathrm{m}$. First, the values of velocity on the grid $200 \times 200 \times 200\,\mathrm{m}$ were chosen from the original dense grid and they were inverted into the values of slowness. We call this data as "chosen". Second, the values of velocity were chosen on the grid $40 \times 40 \times 40\,\mathrm{m}$, inverted into the values of slowness, and the slowness on the grid $200 \times 200 \times 200\,\mathrm{m}$ was computed by arithmetical averaging from the slowness on the grid $40 \times 40 \times 40\,\mathrm{m}$, analogously as the data for the smooth version of the Salt Model. We call this data as "averaged". The third kind of the data is similar to the first one, but the artificial layers, modelled by the velocity step of 15 % and serving as reflectors for migrations (Aminzadeh *et al.* 1997), were removed from the velocity field. The fourth kind of the data is similar to the second kind, again without the artificial thin layers. The results of the test, shown in Table 7, demonstrate that the "chosen" slownesses provide better results than the "averaged" slownesses, and that the removal of the artificial thin layers improves the results of the inversion.

data grid / data grid intervals	model spline grid / model spline intervals	$\frac{S_u}{\mathrm{m}^3\,\mathrm{s}^{-1}}$	$\frac{\|u\|}{(\mathrm{s\,m}^{-3}\ 10^{-9})}$	$\frac{\lvert\frac{v-v_0}{v_0}\rvert}{(\%)}$	$\frac{\lvert\frac{u-u_0}{u_0}\rvert}{(\%)}$	$\frac{\lvert v-v_0\rvert}{(\mathrm{m\,s}^{-1})}$	$\frac{\lvert u-u_0\rvert}{(\mathrm{s\,m}^{-1}\ 10^{-4})}$
68×68×20 / 200×200×200	5×5×3 / 3500×3500×∼1700	0	0.183	5.53	6.13	146	0.213
46×46×14 / 300×300×300	5×5×3 / 3500×3500×∼1700	0	0.165	5.74	6.34	151	0.223
34×34×20 / 400×400×200	5×5×3 / 3500×3500×∼1700	0	0.183	5.51	6.08	145	0.212
23×23×20 / 600×600×200	5×5×3 / 3500×3500×∼1700	0	0.190	5.59	6.19	147	0.216
17×17×20 / 800×800×200	5×5×3 / 3500×3500×∼1700	0	0.195	5.66	6.27	149	0.219
11×11×20 / 1340×1340×200	5×5×3 / 3500×3500×∼1700	0	0.177	5.63	6.30	148	0.220
17×17×20 / 800×800×200	8×8×9/8 / 2000×2000×250	10000	0.294	5.45	5.83	143	0.203
17×17×39 / 800×800×100	8×8×9/8 / 2000×2000×250	10000	0.257	5.24	5.69	137	0.196
11×11×20 / 1340×1340×200	8×8×9/8 / 2000×2000×250	10000	0.363	5.63	6.96	146	0.211
11×11×20 / 1340×1340×200	10×10×10/9 / 1500×1500×220	10000	0.468	6.03	6.17	155	0.223
11×11×20 / 1340×1340×200	10×10×10/9 / 1500×1500×220	25000	0.199	5.53	5.86	143	0.208

Table 6: Results of the inversion in the Salt Model in dependence on the grid dimensions of the data used for the P-wave velocity and in dependence on the parameterization of the velocity field in the model. The interfaces are described by the same functions in all the models.

If the data for the inversion represent a smooth function to be modelled, and if they do not contain any noise, it is much better to use the "chosen" data than the "averaged" data. For example, if we imagine a smooth one–dimensional function represented by a set of points, the "chosen" points always represent the functional values, but the "averaged" points are shifted from the functional values in the direction of the second derivatives. The artificial thin layers in the Salt Model may be thus understood as a noise of the smooth velocity function, and the best results are obtained if we remove this noise and if we use the "chosen" slowness data instead of the "averaged" slowness data.

	$\frac{S_u}{\mathrm{m}^3\,\mathrm{s}^{-1}}$	$\frac{\|u\|}{(\mathrm{s\,m}^{-3}\ 10^{-9})}$	$\frac{\lvert\frac{v-v_0}{v_0}\rvert}{(\%)}$	$\frac{\lvert\frac{u-u_0}{u_0}\rvert}{(\%)}$	$\frac{\lvert v-v_0\rvert}{(\mathrm{m\,s}^{-1})}$	$\frac{\lvert u-u_0\rvert}{(\mathrm{s\,m}^{-1}\ 10^{-4})}$
slowness chosen	0	0.183	5.53	6.13	146	0.213
slowness averaged	0	0.204	7.04	7.96	182	0.296
slowness chosen, no layers	0	0.190	5.38	5.99	142	0.207
slowness averaged, no layers	0	0.180	6.71	7.65	176	0.280

Table 7: Results of the inversion in the Salt Model in dependence on the kind of the data used for the velocity inversion. For the description of the kinds of the data see the text.

The best model we obtained (see Table 8) has the standard relative deviation of velocity $|\frac{v-v_0}{v_0}| = 5.11\%$. The Sobolev norm of the slowness field in the model is $0.302\ 10^{-9}\,\mathrm{s\,m}^{-3}$. The "average Lyapunov exponent" of the velocity field in the model is $0.152\,\mathrm{s}^{-1}$. Note that the exponent does not take into account the velocity steps at the structural interfaces.

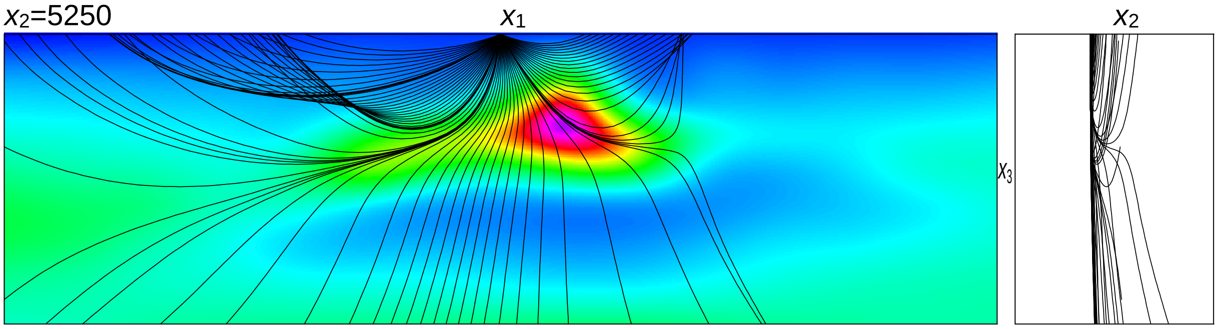

Figure 13: Rays computed by one–parametric shooting of a refracted wave in the $x_1 - x_3$ plane in the smooth version of the Salt Model. The rays are projected onto the $x_1 - x_3$ and onto the $x_2 - x_3$ planes. The coordinates of the point source are [7000,5250,0] m. The $x_1 - x_3$ plane is coloured according to the P-wave velocity in the $x_1 - x_3$ section containing the point source. The colour scale ranges from dark blue for 1500 $\mathrm{m\,s^{-1}}$ in the water to red for 4450 $\mathrm{m\,s^{-1}}$ in the salt body. The horizontal extents of both the $x_1 - x_3$ and $x_2 - x_3$ sections are 14000 m, the vertical extents of the sections are 4200 m. The reader is reminded that the standard relative deviation of the velocity in the model from the data is 8.22%.

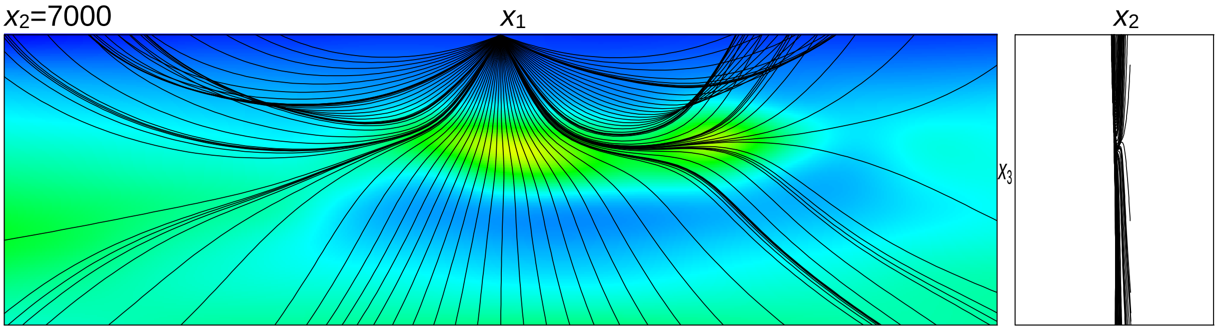

Figure 14: Rays computed by one–parametric shooting of a refracted wave in the $x_1 - x_3$ plane in the smooth version of the Salt Model. The x_2 coordinate of the point source and of the velocity section is now 7000 m. The colour scale is the same as in Figure 13.

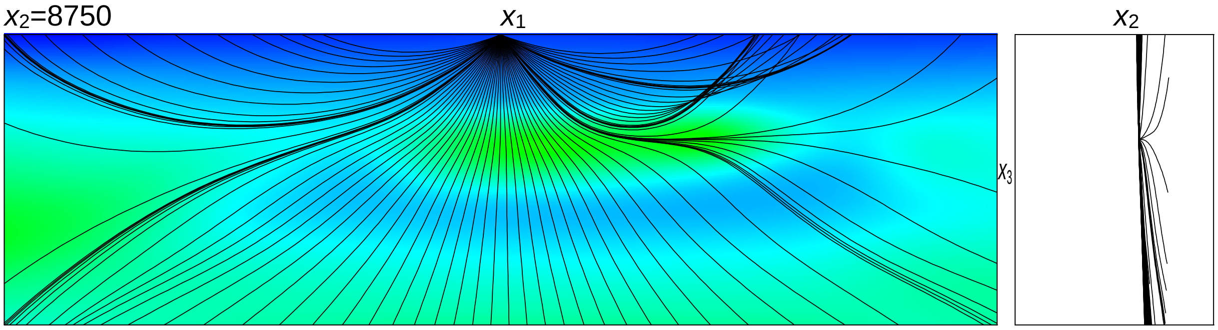

Figure 15: Rays computed by one–parametric shooting of a refracted wave in the $x_1 - x_3$ plane in the smooth version of the Salt Model. The x_2 coordinate of the point source and of the velocity section is 8750 m. The colour scale is the same as in Figure 13.

4.2.6 Tests of ray tracing in the inverted models

We performed several tests of ray tracing in the models obtained after the inversions. As it is difficult to clearly display the results of 3-D ray tracing, we decided to shoot the rays only in the direction of the $x_1 - x_3$ plane (one–parametric shooting in a 3-D model). We then projected the computed rays onto the x_1–x_3 plane and onto the x_2–x_3 plane. The projected rays together with the velocity sections corresponding to the x_2 coordinates of the sources are displayed in Figures 13 to 18.

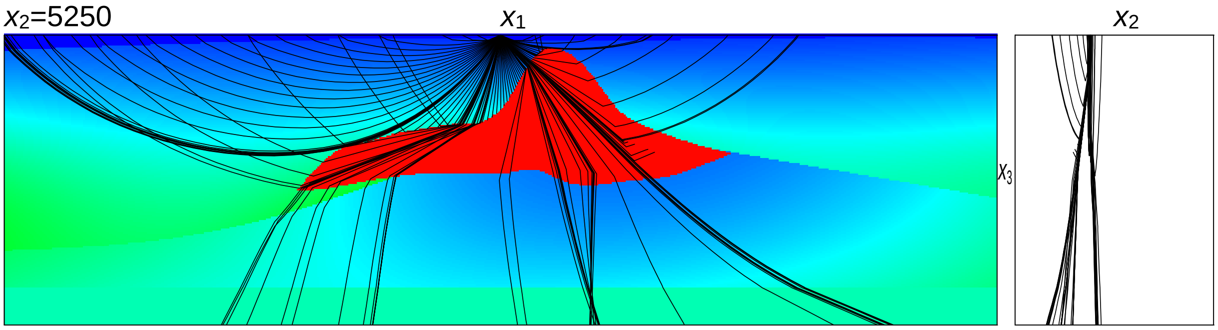

Figure 16: Rays computed by one–parametric shooting of a refracted wave in the $x_1 - x_3$ plane in the Salt Model, the version with interfaces. The x_2 coordinate of the point source and of the velocity section is 5250 m. The colour scale is the same as in Figure 13. The reader is reminded that the standard relative deviation of the velocity in the model from the data is 5.24%.

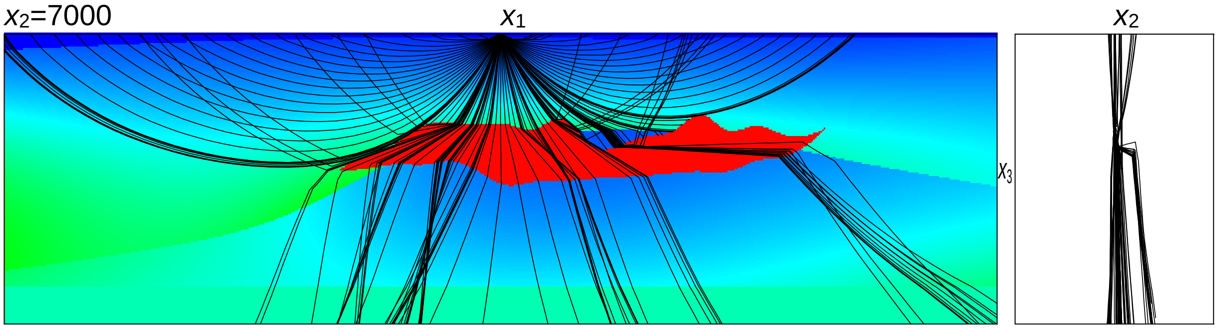

Figure 17: Rays computed by one–parametric shooting of a refracted wave in the $x_1 - x_3$ plane in the Salt Model, the version with interfaces. The x_2 coordinate of the point source and of the velocity section is 7000 m. The colour scale is the same as in Figure 13.

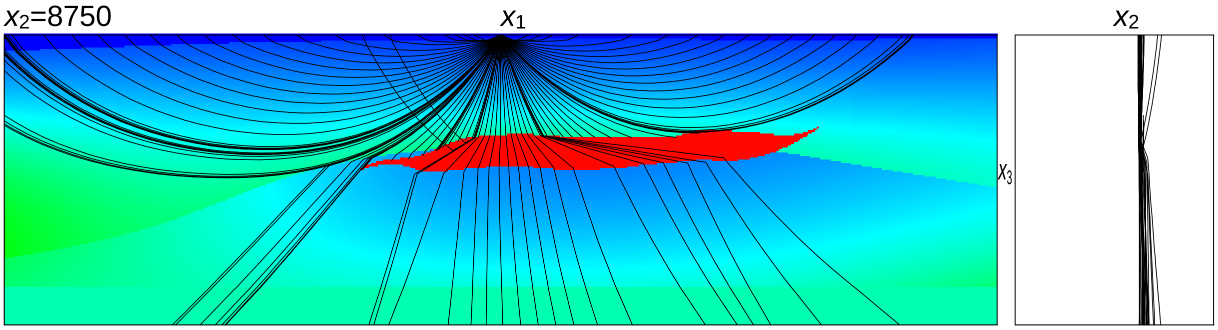

Figure 18: Rays computed by one–parametric shooting of a refracted wave in the $x_1 - x_3$ plane in the Salt Model, the version with interfaces. The x_2 coordinate of the point source and of the velocity section is 8750 m. The colour scale is the same as in Figure 13.

$\frac{S_u}{\mathrm{m^3\,s^{-1}}}$	$\frac{\Vert u \Vert}{(\mathrm{s\,m^{-3}\ 10^{-9}})}$	$\frac{\lvert \frac{v-v_0}{v_0} \rvert}{(\%)}$	$\frac{\lvert \frac{u-u_0}{u_0} \rvert}{(\%)}$	$\frac{\lvert v-v_0 \rvert}{(\mathrm{m\,s^{-1}})}$	$\frac{\lvert u-u_0 \rvert}{(\mathrm{s\,m^{-1}\ 10^{-4}})}$	$\frac{\bar{\lambda}}{(\mathrm{s^{-1}})}$
2500	0.374	5.15	5.75	137	0.197	0.181
5000	0.302	5.11	5.70	136	0.195	0.152
7500	0.256	5.11	5.70	136	0.195	0.133
10000	0.222	5.12	5.70	136	0.195	0.121

Table 8: Results of the inversion in the Salt Model in dependence on the weighting factor S_u. The velocity in the model is parametrized by $8 \times 8 \times 9/8$ points spaced at $2000 \times 2000 \times 250$ m. The values of slowness on the grid of $17 \times 17 \times 39$ points spaced at $800 \times 800 \times 100$ m, calculated from the velocity chosen from the original dense grid with removed artificial thin layers, are used as the data for the inversion.

4.3 Building 2-D model Pluto 1.5 for ray tracing

4.3.1 Data for the model

The grided velocities for 2-D model Pluto 1.5 were created by Smaart Joint Venture, see http://www.smaartjv.com . The P-wave velocities are discretized on a grid of 6960 $\times$ 1201 points with a spacing of 25 ft $\times$ 25 ft. The grid has thus horizontal dimension 173975 feet and vertical dimension 30000 feet. The grid contains three salt bodies of constant velocity. See Figure 19.

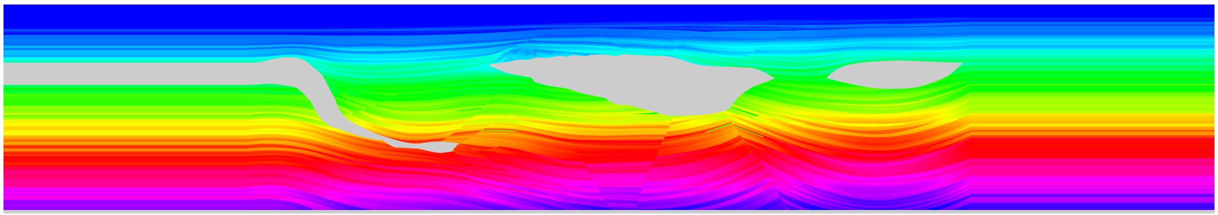

Figure 19: P-wave velocity in the original data grid for model Pluto 1.5. The background velocity varies from 4920 ft s^{-1} at the top of the model to 13580 ft s^{-1} at the bottom. The velocity of the salt bodies is constant and equals 14800 ft s^{-1}. The horizontal dimension of the model is 173975 ft, its vertical dimension is 30000 ft.

We decided to create a model containing the three salt bodies separated by structural interfaces from the continuous background. We calculate the data for the interfaces from the grided velocities by searching for two neighbouring gridpoints, one of them displaying the velocity of the background, and the second one the velocity of the salt. The coordinates of a point of the interface are then taken between such two gridpoints.

We cannot use all the identified points at interfaces and all the gridpoints of the velocity grid as the data for inversion due to the limited memory of our computer. We thus resample the data to several sparser grids, and we use the data on sparser grids as the data for the inversion. We know from the previous experiments with model Hess and with the SEG/EAGE Salt Model that the model spline grid should be about 1.5 sparser than the corresponding data grid. We also know that the memory requirements of the current coding of the method are $M(D+M)$ storage locations, where M is the number of model parameters, and D is the number of data points. We thus take $D \approx 1.5M$ and directly estimate the optimum dimensions of the data and model spline grids which are the maximum grids which may be used on our computer. To be able to estimate the velocity deviation caused by insufficient B-spline sampling of the model, we use also several sparser B-spline and data grids. Figure 20 shows the P-wave velocity and the points at interfaces used as the data for the inversion described below in Chapter 4.3.5 and Table 10.

4.3.2 Model parametrization

We choose the parameterization of the model as follows: for the interfaces we take B–spline grid with spline points regularly spaced in the region of the salt bodies and 2 points at the sides of the model. We use one surface to model the top of the left salt, second surface for the bottom of the left salt, third surface for the top of the middle and of the right salt, and fourth surface for the bottom of the middle and of the right salt.

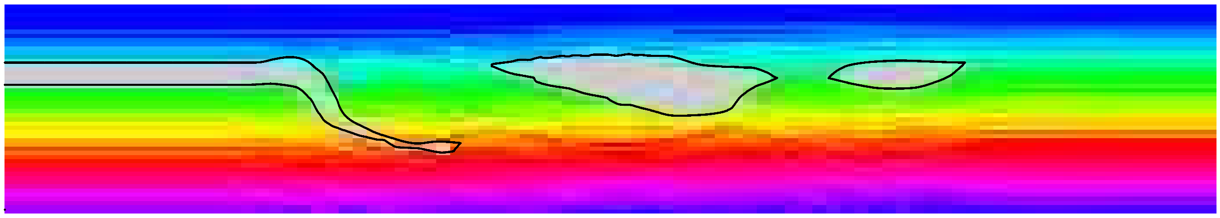

Figure 20: P-wave velocity in the data grid of 50×87 points with a spacing of $600\,\mathrm{ft} \times 2000\,\mathrm{ft}$, plotted together with the points at interfaces identified with the grid spacing of 75 ft. The gridded velocity and the points at interfaces are used as the data for the inversion described in Chapter 4.3.5 and Table 10. The background velocity varies from $4920\,\mathrm{ft\,s^{-1}}$ at the top of the model to $13580\,\mathrm{ft\,s^{-1}}$ at the bottom. The velocity of the salt bodies is constant and equals $14800\,\mathrm{ft\,s^{-1}}$. The points at interfaces are plotted by black dots.

For the background velocity, we take a sparser regular grid of 19×36 spline points with a spacing of $1600\,\mathrm{ft} \times 5000\,\mathrm{ft}$, and a denser regular grid of 38×60 spline points with a spacing of $800\,\mathrm{ft} \times 3000\,\mathrm{ft}$.

4.3.3 Choosing the maximum Lyapunov exponent and the maximum Sobolev norm

The average velocity of the model is $\langle v \rangle = 9902.58\,\mathrm{ft\,s^{-1}}$, the average slowness of the model is $\langle u \rangle = 0.128\;10^{-3}\,\mathrm{s\,ft^{-1}}$. If we consider the maximum sum of the ray paths to be about 100000 ft, we arrive at the estimation that the maximum sum of the travel times from a source and a receiver is limited by $T_{\max} = 12.8\,\mathrm{s}$. Analogously as for model Hess we choose the maximum "average Lyapunov exponent" $\bar{\lambda}_{\max}$ of the model as $\bar{\lambda}_{\max} = \frac{2}{T_{\max}} = 0.156\,\mathrm{s^{-1}}$. The maximum Sobolev norm $\|v\|_{\max}$ of the velocity field in the model chosen according to equation (15) is $\|v\|_{\max} = 0.462\;10^{-4}\,(\mathrm{ft\,s})^{-1}$. Again, we have no quantitative criteria on the smoothness of the structural interfaces.

4.3.4 Inversion of the interfaces

We start the inversion of the interfaces with very sparse data and model spline grids: the grid spacing of the data points at interfaces is 2500 ft, and the interfaces are parametrized by irregular model spline grid with spacing of 5000 ft in the region covered by the data and with two additional points at the model boundary. The initial value of $S_x = 0\,\mathrm{ft}$ is again zero, as in previous models. We then perform the inversion of interfaces for several data and model spline grids. We then for each obtained model perform the same velocity inversion with the sparser B-spline velocity parametrization, and we calculate the standard velocity deviation of the model from the original dense velocity data grid, see Table 9.

data grid intervals/ ft	model spline intervals/ ft	$\lvert\frac{v-v_0}{v_0}\rvert/(\%)$	$\lvert v-v_0\rvert/(\mathrm{ft\,s^{-1}})$
2500	5000	5.00	488.86
1250	2500	4.41	365.40
625	1250	3.34	279.64
250	500	3.30	265.72
75	150	3.26	263.05

Table 9: Results of the inversion of interfaces in model Pluto 1.5 in dependence on the horizontal grid interval of the data points at interfaces and on the horizontal spline interval of the functions describing the interfaces in the constructed model. Velocity field is the same in all the models.

Final step of the inversion of the interfaces is the optimization of the value of S_x. We again have no quantitative criteria on the smoothness of the structural interfaces.

We thus start at $S_x = 0\,\mathrm{ft}$, we increase the value of S_x several times, and we choose the value of S_x which provides the model with minimum standard velocity deviation. The smoothness of the interfaces will be tested by ray tracing.

4.3.5 Inversion of the velocity

We decided to use the values of velocity resampled to the grid of 50×87 points with a spacing of $600\,\mathrm{ft} \times 2000\,\mathrm{ft}$, as the data for velocity inversion. We use the denser model B-spline parametrization of 38×60 spline points with a spacing of $800\,\mathrm{ft} \times 3000\,\mathrm{ft}$. This configuration of the data and model spline grids requires 15116400 storage locations in computer memory, which is almost the maximum amount available on our PC with 64 Mbytes of memory.

The inversion without minimization of the Sobolev norm is ill–conditioned. The inversion with very small weighting factor S_v of the Sobolev norm yields the velocity model which differs from the given velocities by 3.261 %. The "average Lyapunov exponent" of the model is $0.497\,\mathrm{s}^{-1}$, and the behavior of the rays in the model is too chaotic, see Figure 21. When we increase the weighting factor to the value of $S_v = 1000000\,\mathrm{ft\,s}$, we obtain very smooth model with the standard relative velocity deviation 2.706 % and the "average Lyapunov exponent" $0.075\,\mathrm{s}^{-1}$. Figure 25 shows, how the smoothing of the velocity field by including the Sobolev norm in the velocity inversion regularizes the chaotic behaviour of rays. The results of the inversion for different values of S_v are shown in Table 10. For the model with the lowest relative velocity deviation see Figure 22, for remaining two models see Figures 23 and 24.

$S_v/(\mathrm{ft\,s})$	$\lvert\frac{v-v_0}{v_0}\rvert/(\%)$	$\lvert v-v_0\rvert/(\mathrm{ft\,s}^{-1})$	$\lambda/(\mathrm{s}^{-1})$
1000	3.261	263.054	0.497
125000	2.611	205.600	0.258
200000	2.627	206.767	0.199
500000	2.672	212.113	0.116
1000000	2.706	214.784	0.075

Table 10: Results of the inversion of the velocity field in model Pluto 1.5 in dependence on weighting factor S_v of the Sobolev norm used. The velocity field is parametrized by 38×60 spline points with a spacing of $800\,\mathrm{ft} \times 3000\,\mathrm{ft}$. The dimensions of the data grid are 50×87 points with a spacing of $600\,\mathrm{ft} \times 2000\,\mathrm{ft}$. The interfaces are parametrized with spline points interval of 150 ft.

Note that in this example the velocity deviation is probably caused rather by insufficient B-spline sampling then by smoothing.

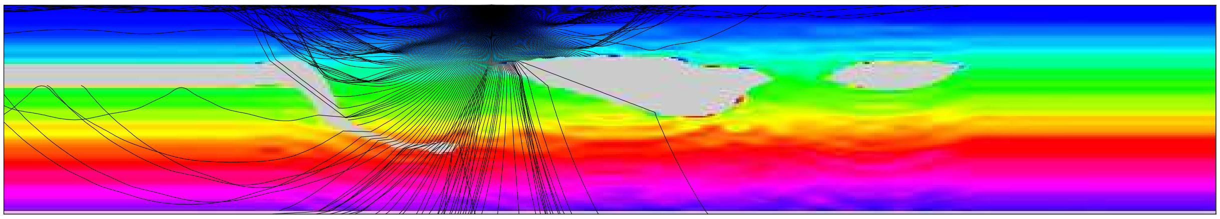

Figure 21: Rays computed by one–parametric shooting in the model Pluto 1.5 obtained after the inversion with $S_v = 1000\,\mathrm{ft\,s}$. The colour scale is the same as in Figure 19. The standard relative deviation of the velocity in the model from the full data grid is 3.261%.

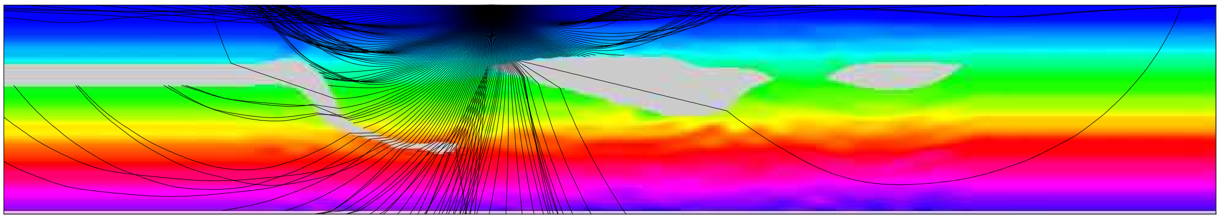

Figure 22: Rays computed by one–parametric shooting in the model Pluto 1.5 obtained after the inversion with $S_v = 125000\,\mathrm{ft\,s}$. The standard relative deviation of the velocity in the model from the full data grid is 2.611%.

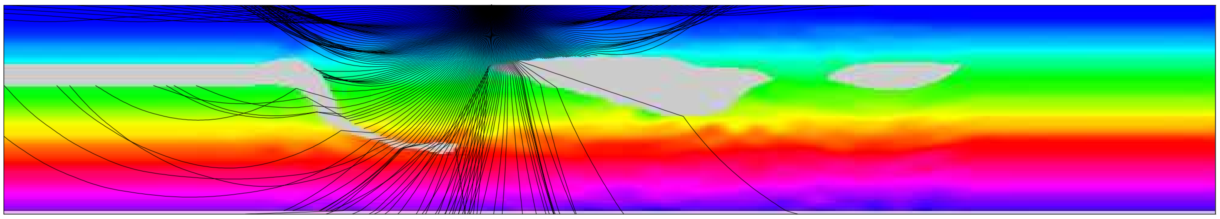

Figure 23: Rays computed by one–parametric shooting in the model Pluto 1.5 obtained after the inversion with $S_v = 200000\,\mathrm{ft\,s}$. The standard relative deviation of the velocity in the model from the full data grid is 2.627%.

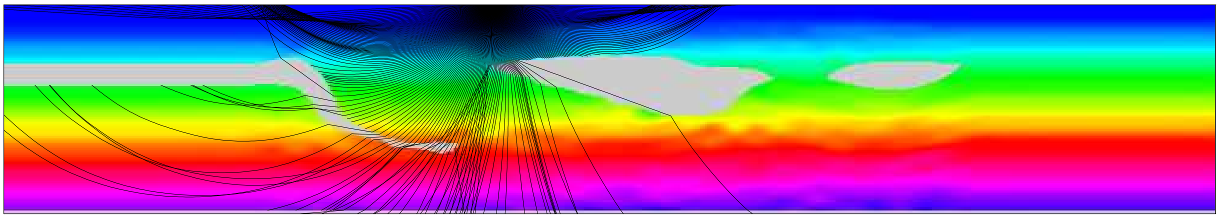

Figure 24: Rays computed by one–parametric shooting in the model Pluto 1.5 obtained after the inversion with $S_v = 500000\,\mathrm{ft\,s}$. The standard relative deviation of the velocity in the model from the full data grid is 2.672%.

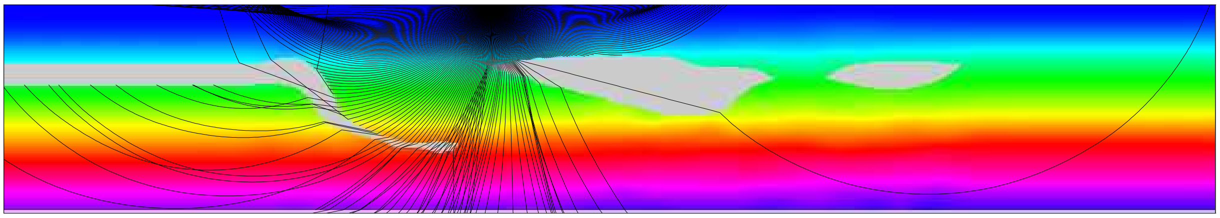

Figure 25: Rays computed by one–parametric shooting in the model Pluto 1.5 obtained after the inversion with $S_v = 1000000\,\mathrm{ft\,s}$. The standard relative deviation of the velocity in the model from the full data grid is 2.706%.

5 Conclusions

The minimization of the Sobolev norm of the model during linearized inversion enables us to control the model parameters unresolved by the data being fitted, while the parameters determined by the data remain almost unchanged. It enables us to minimize not only the difference between the data and the model, but, for many computational methods, also the difference between the exact solution and the results obtained by the considered numerical method to be used.

The smoothness of the velocity field of the models constructed for the ray methods may be quantitatively described in terms of the "average Lyapunov exponent" for the model. The "average Lyapunov exponent" may be approximated by the square root of the corresponding Sobolev norm of the model. This enables us to determine the quantitative criteria on the models, so as to be suitable for ray tracing, in terms of Sobolev scalar products. The criteria then allow us to construct the optimum models of geological structures for ray tracing, either by smoothing given rough models, or by inversion of seismic data.

The numerical examples demonstrate the application of Sobolev norm to the regularization of the ill–conditioned inversion. The behaviour of the model functions in the regions not illuminated by the data is controlled by the Sobolev norm.

The example of smoothing model Hess shows, how the smoothing of the velocity field by including the Sobolev norm in the velocity inversion regularizes the chaotic behaviour of rays, while the velocity field changes only slightly with the standard relative deviation of 1.8 per mille. Note that the standard relative velocity deviation is equivalent to the standard relative travel–time deviation for very short rays.

The example of building the SEG/EAGE Salt Model demonstrates the use of Sobolev norms in inverting 3-D data.

The examples of building the SEG/EAGE Salt Model and of building model Pluto 1.5 pointed out the weakness of the current coding of the method, which is its extremal memory demand.

Acknowledgements

This research has been supported by the Grant Agency of the Czech Republic under Contract 205/01/0927, by the Ministry of Education of the Czech Republic within Research Project J13/98 113200004, and by the members of the consortium "Seismic Waves in Complex 3-D Structures", see http://seis.karlov.mff.cuni.cz/consort/main.htm . The data for model Hess have been provided by Scott Morton of the Amerada Hess Corporation. The author expresses his thanks to Luděk Klimeš for his kind guidance of the work being presented in the paper, and to Ivan Pšenčík and both anonymous reviewers for their comments and suggestions resulting in substantial improvement of the paper.

References

Aminzadeh, F., Brac, J., Kunz, T. (1997): 3-D Salt and Overthrust Models. SEG/EAGE 3-D Modeling Series No.1., Soc. Explor. Geophysicists, Tulsa.

Bulant, P. (2000): Smoothing 2-D model HESS for Kirchhoff migrations. In: Seismic Waves in Complex 3-D Structures, Report 10, pp. 75–82, Department of Geophysics, Charles University, Prague.

Bulant, P. (2002): Sobolev scalar products in the construction of velocity models – application to model Hess and to SEG/EAGE Salt Model. Pure and appl. Geophys., **159**, in press.

Červený, V., Klimeš, L. & Pšenčík, I. (1988): Complete seismic–ray tracing in three–dimensional structures. In: Doornbos, D.J. (ed.), Seismological Algorithms, pp. 89–168, Academic Press, New York.

Grubb, H.J. & Walden, A.T. (1995): Smoothing seismically derived velocities. Geophys. Prosp., **43**, 1061–1082.

Klimeš, L. & Kvasnička, M. (1994): 3-D network ray tracing. Geophys. J. int., **116**, 726–738.

Klimeš, L. (1996): Grid travel–time tracing: second–order method for the first arrivals in smooth media. PAGEOPH, **148**, 539–563.

Klimeš, L.: (2000a): Sobolev scalar products in the construction of velocity models. In: Seismic Waves in Complex 3-D Structures, Report 10, pp. 15–40, Dep. Geophys., Charles Univ., Prague, online at http://seis.karlov.mff.cuni.cz/consort/main.htm .

Klimeš, L.: (2000b): Smoothing the Marmousi model for Gaussian–packet migrations. In: Seismic Waves in Complex 3-D Structures, Report 10, pp. 63–74, Dep. Geophys., Charles Univ., Prague, online at http://seis.karlov.mff.cuni.cz/consort/main.htm .

Klimeš, L. (2000c): Lyapunov exponents for 2-D ray tracing without interfaces. Expanded Abstracts of 70th Annual Meeting (Calgary), pp. 2293–2296, Soc. Explor. Geophysicists, Tulsa.

Klimeš, L. (2002a): Application of the medium covariance functions to travel–time tomography. Pure and appl. Geophys., in press.

Klimeš, L. (2002b): Lyapunov exponents for 2-D ray tracing without interfaces. Pure and appl. Geophys., in press.

Podvin, P. & Lecomte, I. (1991): Finite difference computation of traveltimes in very contrasted velocity models: a massively parallel approach and its associated tools. Geophys. J. int., **105**, 271–284.

Pretlová, V. (1976): Bicubic spline smoothing of two–dimensional geophysical data. Studia geophys. geod., **20**, 168–177.

Pretlová, V. (1985): Bicubic spline smoothing of the data given at points of a rectangular network. Studia geophys. geod., **29**, 238–247.

Tarantola, A. (1987): Inverse Problem Theory. Elsevier, Amsterdam.

Versteeg, R.J. (1991): Analysis of the problem of the velocity model determination for seismic imaging. PhD thesis, University of Paris VII.

Žáček, K. (2002): Smoothing the Marmousi model. Pure and Applied Geophysics, in press.